

Supporting Information for

Tilting and twisting in a novel perovzalate, $\text{K}_3\text{NaMn}(\text{C}_2\text{O}_4)_3$

Xiaolong He,^{a,d,‡} Xinyuan Zhang,^{c,‡} Bifa Ji,^{a,e,‡} Wenjiao Yao,^{a,} Philip Lightfoot,^{b,*}*

Yongbing Tang^{a,d,e,f}*

^a Functional Thin Films Research Center, Shenzhen Institutes of Advanced Technology, Chinese Academy of Sciences, Shenzhen 518055, China. E-mail: wj.yao@siat.ac.cn; tangyb@siat.ac.cn

^b School of Chemistry and EaStChem, University of St Andrews, St Andrews, Fife KY16 9ST, UK. E-mail: pl@st-andrews.ac.uk

^c Tianjin Key Laboratory of Functional Crystal Materials, Institute of Functional Crystals, Tianjin University of Technology, Tianjin 300384, China.

^d Nano Science and Technology Institute, University of Science and Technology of China, Suzhou 215123, China.

^e Shenzhen Institute of Advanced Technology, University of Chinese Academy of Sciences, Shenzhen 518055, China.

^f Key Laboratory of Advanced Materials Processing & Mold, Ministry of Education, Zhengzhou University, Zhengzhou 450002, China.

E-mail: wj.yao@siat.ac.cn; pl@st-andrews.ac.uk; tangyb@siat.ac.cn

KEYWORDS: oxalate, perovskite, crystal structure.

Table of Content

1. Materials and Synthesis
2. Atomic parameters and key bond lengths for **1**
3. Shelx refinement in space group $Ia\bar{3}d$.
4. Figure S1. Rietveld refinement on powder XRD for **1**
5. Figure S2. Simulated powder XRD for ordered and disordered Mn/Na sites.
6. Figure S3. Thermal stability and an optical image.
7. Figure S4. Comparison of different nets.

Materials and Synthesis

Alkali metal carbonate (Na_2CO_3 , K_2CO_3 , 99%), manganese (II) chloride tetrahydrate ($\text{MnCl}_2 \cdot 4\text{H}_2\text{O}$, 98%), and oxalic acid dihydrate ($\text{H}_2\text{C}_2\text{O}_4 \cdot 2\text{H}_2\text{O}$, 99%) were purchased from Sigma Aldrich. All chemicals were applied directly without further treatment. Reactants in the molar ratio of Na_2CO_3 : K_2CO_3 : $\text{MnCl}_2 \cdot 4\text{H}_2\text{O}$: $\text{H}_2\text{C}_2\text{O}_4 \cdot 2\text{H}_2\text{O}$ = 4:8:4.5:12 were weighed and mixed thoroughly in an agate mortar by hand ground before transferring to Teflon-lined stainless steel autoclaves (40 mL), followed by addition of a 1 g distilled water as solvent. The autoclaves were then sealed and put into ovens at 493 K for seven days. After reactions, the oven was turned off and cooled to room temperature. Products were then taken out from autoclaves, filtered with distilled water, and dried overnight in an oven at 80 °C.

Table S1. Atomic parameters and key bond lengths for $\text{K}_3\text{NaMn}(\text{C}_2\text{O}_4)_3$ (Laue class $m\bar{3}$, space group $Ia\bar{3}$ (No. 206), $a = 13.4567(3)$ Å)

Atom	Wyck.	Site	x/a	y/b	z/c	U [Å ²]
Mn1	8a	-.3.	1/2	1/2	1/2	0.00505(14)
K1	24d	2..	1/2	1/4	0.63560(3)	0.00806(13)
Na1	8b	-.3.	3/4	1/4	1/4	0.0069(3)
O1	48e	1	0.53589(7)	0.34822(7)	0.46137(7)	0.00926(19)
O2	48e	1	0.59293(7)	0.30378(7)	0.31134(7)	0.0104(2)
C1	48e	1	0.53716(8)	0.29375(8)	0.38451(8)	0.0056(2)
Bond	Length (Å)	Multiplicity	Bond	Length (Å)	Multiplicity	
Mn1-O1	2.162(2)	6	K1-O2	2.771(3)	2	
C1-O1	1.267(8)	1	K1-O1	2.935(8)	2	
C1-O2	1.245(4)	1	K1-O2	2.825(4)	2	
C1-C1	1.544(9)	1	Na1-O2	2.381(7)	6	
K1-O1	2.734(4)	2				

Structural analysis in space group $Ia\bar{3}d$:

As the checkcif process indicated potential space group $Ia\bar{3}d$ (Laue class $m\bar{3}m$), we rechecked the single crystal XRD data using Shelx refinement. **The R_{merge} and R_1 values for diffraction data are 0.034 and 0.037 for Laue class $m\bar{3}$, and 0.368 and 0.381 for Laue class $m\bar{3}m$.** This clearly shows the Laue class $m\bar{3}$ to be more appropriate. The employment of Laue class $m\bar{3}m$ to the first-step structural determination gave unreasonable results.

In the second trial, we started from space group $Ia\bar{3}$ and the atomic positions in Table S1, adding PART and FVAR instructions to allow mixed Mn/Na occupancy in the 8a and 8b positions. After the refinement, the FVAR showed a value of ~ 1.0 (1.00843), demonstrating the Mn and Na locate solely at 8a and 8b positions, respectively. Thus, the disorder of Mn and Na are excluded in this case.

In another attempt, we applied $Ia\bar{3}d$ symmetry and explicitly defined mixed 50/50 occupancy of Mn and Na. This resulted in 0.1038, 0.318 and 3.834 for R , wR and GOOF, respectively. Meanwhile, two NDP are observed at the Mn/Na sites. Therefore, this attempt of refinement using the $Ia\bar{3}d$ space group also failed.

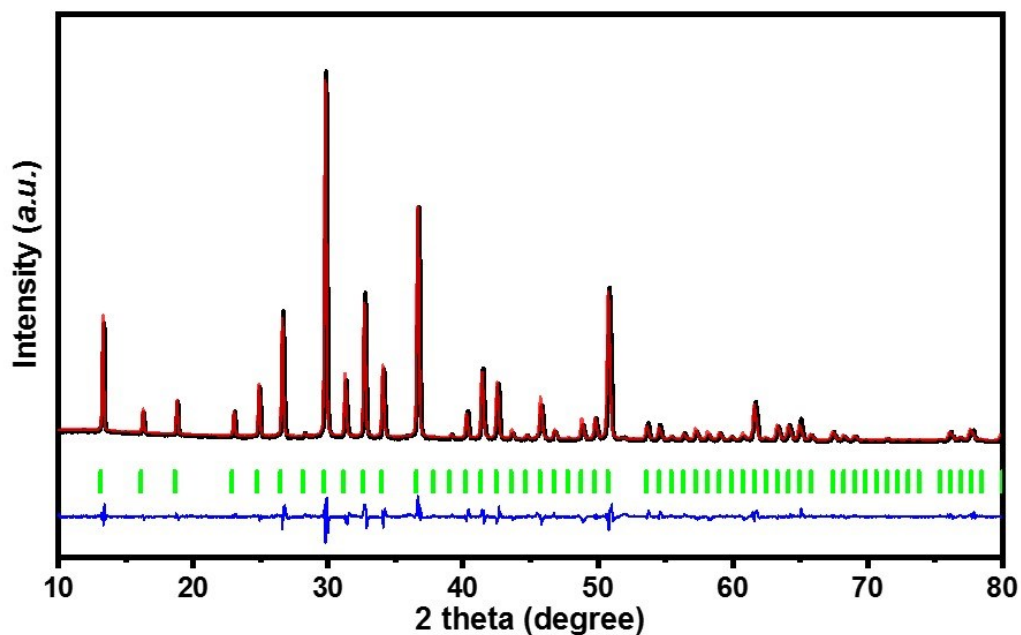


Figure S1. Rietveld refinement on the powder XRD of **1**. Space group $Ia\bar{3}$ (No. 206), $a = 13.391(2)$ Å, $R_p = 0.0727$, $wR_p = 0.0975$, $\chi^2 = 2.016$. Data were collected on a Miniflex 600 Rigaku powder X-ray diffractometer using Cu $K\alpha$ radiation ($\lambda = 1.540598$ Å) at room temperature with a scan step width of 0.05° and a fixed time of 0.2 s. Red, black, and blue lines stand for calculated values, experimental values, and their differences, respectively. Green bars stand for theoretical diffraction positions.

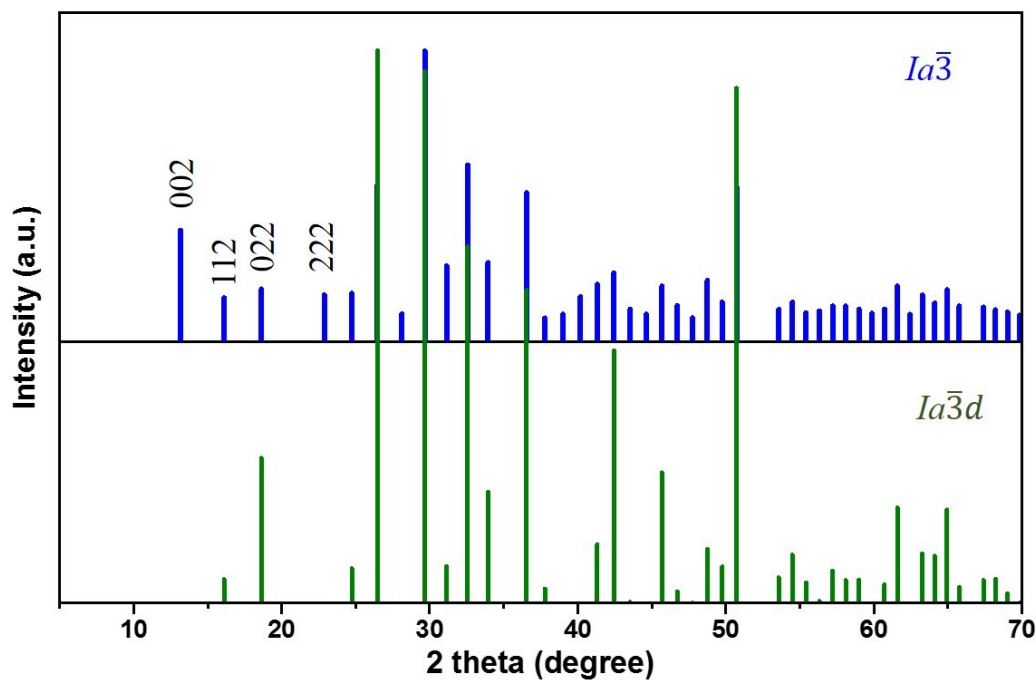


Figure S2. Comparison of theoretical powder XRD of **1** in $Ia\bar{3}$ (blue) and $Ia\bar{3}d$ (green) space group. In $Ia\bar{3}d$ space group, the Mn/Na are required to occupy ‘ $\bar{3}$.’ sites equally in Table S1. Comparing the two patterns, it is obvious that the relative intensity of (112) and (022) peaks are quite different for ordered and disordered ‘ $\bar{3}$.’ sites. Moreover, the systematic absences due to the d -glide ($hhl, 2h+l = 4n$) are clearly observed in the experimental pattern, Figure S1: for example the (002) and (222) reflections near 13° and 23° . Meanwhile, the experimental XRD (Fig S1) agrees with that of ordered ‘ $\bar{3}$.’ sites better than disordered ‘ $\bar{3}$.’ sites.

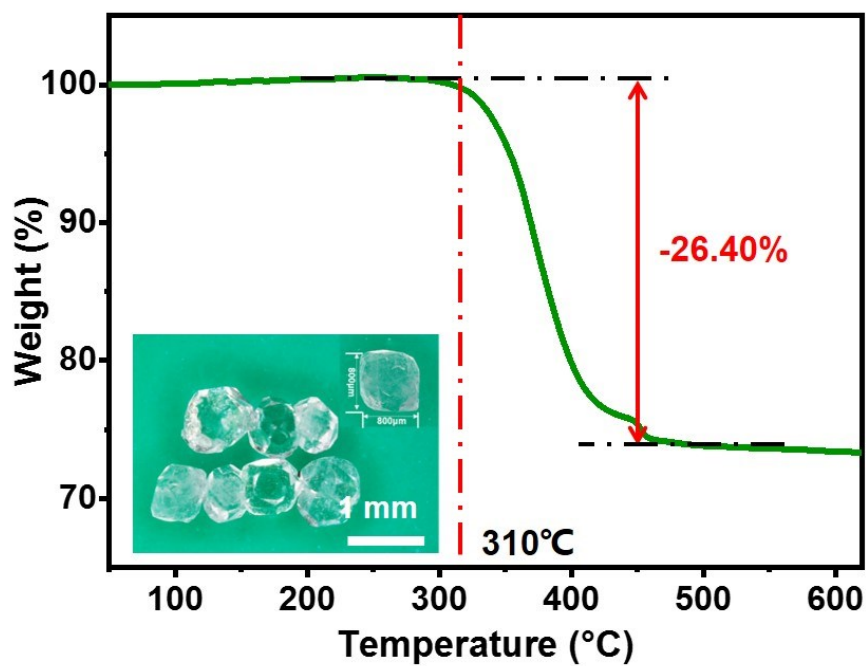


Figure S3. Thermal stability of hand-ground **1** crystallites of about 8 mg by thermogravimetric calorimetry (TG) using a STA449F3 thermal analyzer (Netzsch, Germany) under a flow of nitrogen gas at a rate of $10\text{ }^{\circ}\text{C min}^{-1}$. The inset is an optical image taken by Leica DVM6M video microscope with ultra-depth-of-field.

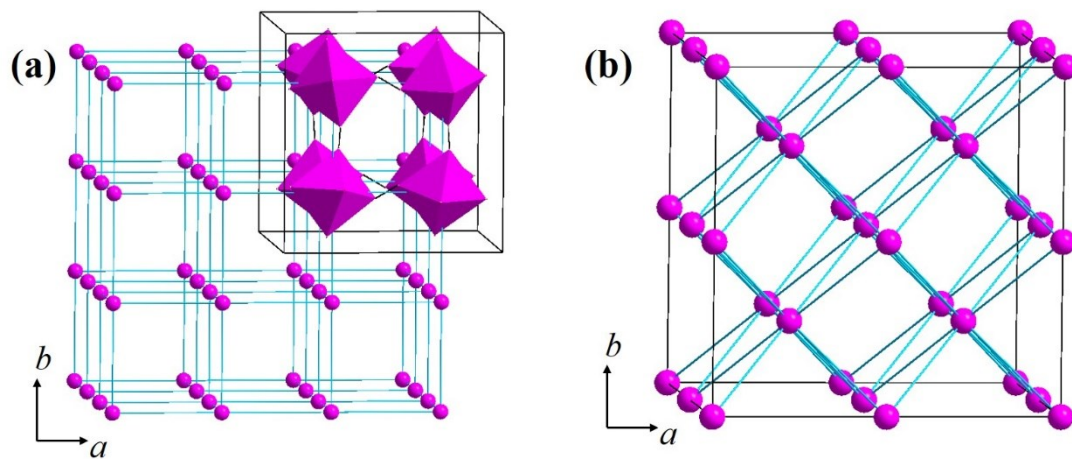


Figure S4. Comparison of idealized *pcu* (a), *bcs* (b) nets in **1**.